

# Observation of Stripe Superstructure in the $\beta$ -Two-Phase Coexistence Region of Cholesterol–Phospholipid Mixtures in Supported Membranes

Seyed R. Tabaei,<sup>†,‡</sup> Joshua A. Jackman,<sup>†,‡</sup> Bo Liedberg,<sup>†,‡</sup> Atul N. Parikh,<sup>\*,†,‡,¶</sup> and Nam-Joon Cho<sup>\*,†,‡,§</sup>

<sup>†</sup>School of Materials Science and Engineering, <sup>‡</sup>Centre for Biomimetic Sensor Science, and <sup>§</sup>School of Chemical and Biomedical Engineering, Nanyang Technological University, 50 Nanyang Avenue, Singapore 639798

<sup>¶</sup>Departments of Biomedical Engineering and Chemical Engineering & Materials Science, University of California, Davis, California 95616, United States

## Supporting Information

**ABSTRACT:** Visualization of phase coexistence in the  $\beta$  region of cholesterol–phospholipid mixtures consisting of high cholesterol concentrations has proved elusive in lipid bilayers. Here, using the solvent-assisted lipid bilayer approach to prepare supported membranes with high cholesterol fractions close to the cholesterol solubility limit, we report the observation of coexisting liquid phases using fluorescence microscopy. At  $\sim 63$  mol % cholesterol, supported membranes consisting of mixtures of DOPC and cholesterol exhibit large-area striping reminiscent of the stripe superstructures that characterize the proximity of the second critical point in the miscibility phase diagram. The properties of the two phases are consistent with condensed complex-rich and cholesterol-rich liquids. Both phases exhibit long-range lateral mobility, and diffusion through a given phase is favored over hopping across the phase boundary, producing an “archipelago effect” and a complex percolation path.

Termed the “condensing effect,” the nonideal mixing of cholesterol (Chol) and phospholipids first reported in 1925 by Leathes has led to an extensive search for regions of liquid–liquid immiscibility in their equilibrium phase diagrams.<sup>1</sup> A significant finding in this regard is the discovery of two upper liquid–liquid miscibility critical points for monomolecular mixtures of Chol and phospholipids at the air–water interface.<sup>1d–f</sup> The corresponding pairs of two-phase coexistence regions, labeled  $\alpha$  for low Chol concentrations ( $\sim 12$ – $28$  mol % Chol) and  $\beta$  for higher Chol concentrations ( $\sim 30$ – $75$  mol % Chol), are often described in terms of a thermodynamic model that invokes the formation of “condensed complexes.”<sup>1c,d,g</sup> In the  $\alpha$  region, phospholipid-rich and condensed complex-rich phases are thought to coexist, and the  $\beta$  region is characterized by the coexistence of the condensed complex-rich and Chol-rich liquids. Although the two-phase coexistence of the monolayer  $\alpha$  region has been reproduced previously in bilayer configurations (e.g., giant vesicles and supported membranes) and the resulting domain patterns have been characterized, efforts to visualize phase coexistence associated with liquid–liquid immiscibility in the  $\beta$  region have proved elusive, probably as a result of challenges in

preparing bilayers containing high concentrations of Chol near the soluble limit.<sup>2</sup>

A dominant method to prepare supported membranes containing requisite high cholesterol concentration to reproduce the  $\beta$  region involves two successive transfers of lipid monolayers. In this approach, it is difficult to produce equilibrated bilayer phases,<sup>3</sup> as revealed by the lack of alignment between domains across the two leaflets,<sup>3a</sup> producing differences in the phase and structural behaviors of monolayers and bilayers.<sup>3c</sup> The surface-mediated fusion of small unilamellar vesicles (SUVs) ( $\sim 100$  nm in diameter) provides an alternate route, but SUVs composed of high fractions of cholesterol are difficult to prepare by standard methods (i.e., extrusion or sonication), presumably because of artifactual demixing.<sup>4</sup>

To this end, the solvent-assisted lipid bilayer (SALB) formation technique is particularly attractive. As first described by Rädler and co-workers and adapted more recently into a continuous solvent-exchange process using a microfluidic setup by our group, the SALB method<sup>5</sup> begins with the lipid deposition onto a solid surface in alcohol. The gradual replacement of alcohol by water drives the formation of supported bilayers at the aqueous interface of buried solid surfaces through an equilibrium structural transition.<sup>5</sup> Implementing this approach using binary mixtures of the phospholipid 1,2-dioleoyl-*sn*-glycero-3-phosphocholine (DOPC) and Chol in the vicinity of the critical concentrations for the  $\beta$  region, we found that the resulting supported membranes exhibit stripe superstructures reminiscent of that found near the critical points in the phase diagram.<sup>1b,6</sup>

For SALB experiments, mixtures of lipids and Chol dissolved in isopropanol were incubated on a glass surface, and the solvent was gradually replaced by introducing Tris buffer (150 mM NaCl, 10 mM Tris, pH 7.4) in a flow-through sample chamber and washing (10 $\times$ ) with excess buffer to remove residual isopropanol. Within minutes of buffer introduction, uniform fluorescence intensity characterizes the substrate-bound membrane when only DOPC is used as the lipid (see Figure S1 in the Supporting Information (SI)). The DOPC bilayer so formed exhibits a uniform structure and lateral fluidity ( $\sim 2.5 \mu\text{m}^2 \text{s}^{-1}$ ) in fluorescence recovery after

Received: August 12, 2014

Published: November 17, 2014

photobleaching (FRAP) measurements, which is in good agreement with well-formed supported DOPC membranes produced by vesicle fusion.<sup>4a</sup> In sharp contrast, when a 4:6 mixture of DOPC and Chol is used, the resulting bilayers reveal a rapidly evolving fluorescence microstructure (Figure 1 and video S1 in the SI), which is described in turn below.

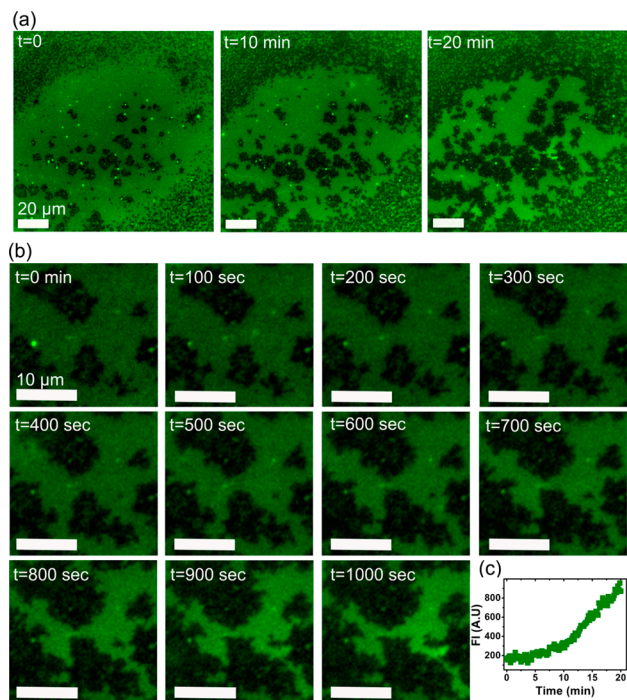


**Figure 1.** Structure formation in a SALB consisting of DOPC and Chol (4:6 molar ratio containing 0.5% rhodamine-PE). (a) Time-lapse Fluorescence images. (b) Corresponding images for an enlarged section of (a). (c) Fluorescence intensity of a typical region within the bright area over time.

The structural evolution, which lasts for 15–20 min, consists of (1) the appearance and rapid growth of irregularly shaped “dark” features exhibiting reduced fluorescence (Figure 1b) and (2) a concomitant increase in the fluorescence intensity from the bright phase (Figure 1c). It is noteworthy that the dark features are not completely devoid of fluorophores (see below) but rather represent the appearance of a dense phase containing reduced concentrations of the fluorophore. This slow time scale of the structural evolution is not surprising: it reflects the gradual exchange of isopropanol, which is necessary for the equilibrium transitions in the bulk from the monomeric-inverted micellar state to the micellar and ultimately the vesicular state.<sup>5a,7</sup> In our case, this is afforded by the low exchange rates in the microfluidic chamber ( $\sim 10$  s), further delayed by the removal of any trapped solvent in the surface-bound bilayer ( $\sim 60$  s).

The ensuing formation of the well-hydrated lipid bilayer then reveals a phase separation of two coexisting phases characterized by a dramatic labyrinthine pattern that consists of microscopic patterns of thin, serpentine features uniformly covering large areas of the lipid bilayer across the substrate surface (Figure 2). Because rhodamine-PE lipid is known to be excluded from cholesterol-rich domains, the observed pattern of dark and bright fluorescence can be assigned to cholesterol-enriched and cholesterol-depleted phases, respectively.

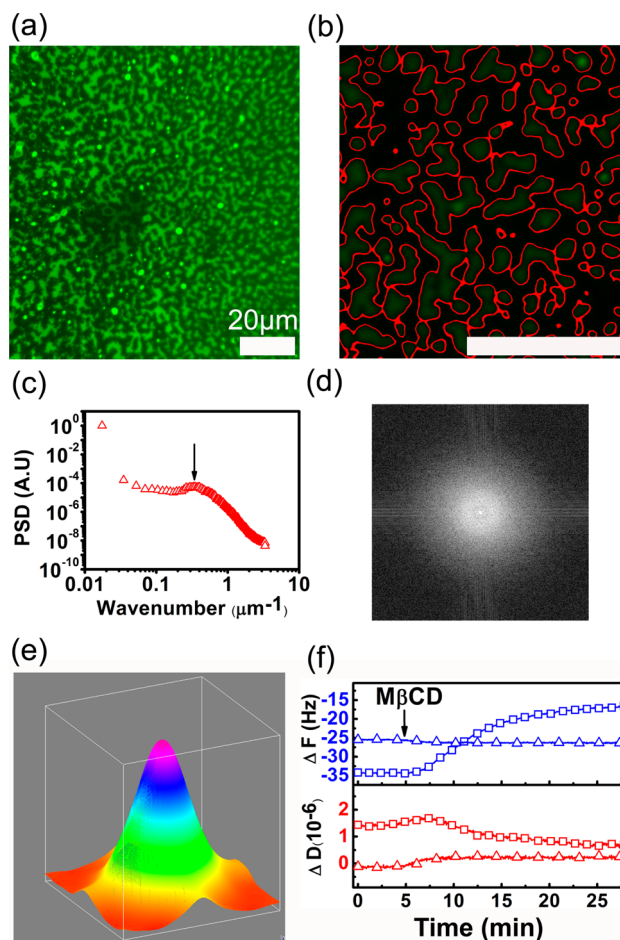


**Figure 2.** Stripe pattern in the supported lipid bilayer with elevated cholesterol in the  $\beta$  phase. (a) Wide-field fluorescence image and (b) an enlarged view revealing the striping. (c) Power spectral density and (d) Fourier transform image of the network. (e) Intensity of the Fourier transform image, showing a Gaussian distribution. (f) QCM-D frequency ( $\Delta F$ ) and dissipation ( $\Delta D$ ) shifts of bilayers formed by the SALB method after the addition of 1 mM methyl- $\beta$ -cyclodextrin (M $\beta$ CD) to 40:60 ( $\square$ ) and 100:0 ( $\triangle$ ) DOPC/Chol mixtures. The arrow indicates the injection time for 1 mM M $\beta$ CD.

The presence of extensive interfaces is indicative of low line tension between the coexisting phases, suggesting proximity to a miscibility critical point.<sup>1h,6a,b</sup> To acquire a quantitative understanding of the nature of the observed stripelike superstructures, we calculated the characteristic length scale of the network ( $L_{\text{network}}$ ) following Subramaniam et al.<sup>8</sup>  $L_{\text{network}}$  is a measure of the dominant length scale of the structures found in an inhomogeneous network. The image of a network with a characteristic length scale exhibits one or two pronounced peaks in its power spectral density (PSD).  $L_{\text{network}}$  is defined as the reciprocal of the wavenumber corresponding to the peak. The PSD of the stripes shows a pronounced peak at a wavenumber of  $0.35 \mu\text{m}^{-1}$ , corresponding to a dominant length scale of  $3.5 \pm 1.4 \mu\text{m}$  ( $n = 6$ ) (Figure 2c). The Fourier transform image of the network reveals a circular pattern and a Gaussian distribution, which confirms the disordered and unoriented nature of the stripe patterns (Figure 2d,e).

The observed coexisting fluid–fluid phases are reminiscent of those observed in the  $\beta$  region in the phase diagram of monolayers of phospholipids at a high mole fraction of cholesterol at the air–water interface.<sup>1c,d</sup> In this region, fluid

domains enriched in Chol–phospholipid complexes coexist with a cholesterol-rich phase.<sup>1d–f</sup> In our case, the complex-enriched domains are identified as bright domains on a dark Chol-rich background.

To further validate that the observed striplike morphology indeed arises from proximity to the second upper critical point, additional experiments demonstrating scale invariance in the compositional fluctuations are needed.<sup>1h,6a,c</sup> The absence of large-scale temporal fluctuations in our case might reflect possible hindrance by the underlying substrate when the equilibrated bilayers become immobilized. Consistent with this picture, elevating the ambient temperature to  $\sim 60$  °C, near the apparent transition temperature, did not perturb the domain pattern (video S2 in the SI).

To confirm that the DOPC:Chol molar ratio in the surface-bound membrane is close to the molar ratio of 4:6 used in the precursor lipid mixture, we measured the Chol content in the supported bilayer using a Chol extraction assay with methyl- $\beta$ -cyclodextrin (M $\beta$ CD), which at low concentrations (<5 mM) selectively removes Chol from lipid bilayers.<sup>9</sup> We quantified the amount of Chol extracted from the supported bilayer using quartz crystal microbalance dissipation (QCM-D) measurements,<sup>10</sup> which track the global adsorption/desorption kinetics of a deposited material (in this case, the lipid bilayer) on a substrate (Figure 2f and Figure S2 in the SI). Following the injection of 1 mM M $\beta$ CD over the supported membrane, the frequency increases with time, consistent with the loss of mass due to the removal of cholesterol (Figure 2f, blue trace). From these data, the concentration of Chol in the bilayer was estimated to be  $\sim 63$  mol % using the Sauerbrey relationship.<sup>10b</sup> This value is near the precursor concentration, which we chose to be in the vicinity of the upper critical point for the  $\beta$  region of phase coexistence. As expected, monitoring of fluorescence images during M $\beta$ CD incubation revealed that the stripe pattern dissolves, and the residual membrane displays long-range fluidity in FRAP measurements (video S3 in the SI), which is further consistent with the notion that the observed striping is due to the high-cholesterol  $\beta$ -region phase coexistence.

To verify the long-range fluidity of the coexisting phases, we monitored the diffusion of a fluorescent lipid in both domains using FRAP (Figure 3). As expected, the fluorescent tracer is laterally mobile in each of the two coexisting phases. The dark phase exhibits nearly complete recovery, and the fluorescence intensity within the partially bleached domains exhibits limited recovery (Figure 3c), the latter indicating that there is lateral fluidity within single domains and that the bright domains represent a discrete, unconnected phase. The FRAP image sequence also shows that the dark phase (which is denser) acts as a field of mobile and semipermeable obstacles for the diffusion of single lipids (Figure 3d). Thus, while the fluorescent tracer is laterally mobile in each of the two phases,<sup>11</sup> diffusion through a given phase appears to be favored over hopping across the phase boundaries, producing a characteristic “archipelago effect.”<sup>12</sup>

The quantitative diffusional characteristics of lipids are complicated by the presence of the stripe topography and convoluted diffusion path. At a rudimentary level, with the assumption that the system exhibits normal diffusion, the analysis of the recovery over the photobleached area gives a lateral diffusivity of  $0.3 \mu\text{m}^2 \text{s}^{-1}$ , which is an order of magnitude lower than the lipid diffusivity in a pure DOPC bilayer.<sup>11</sup>

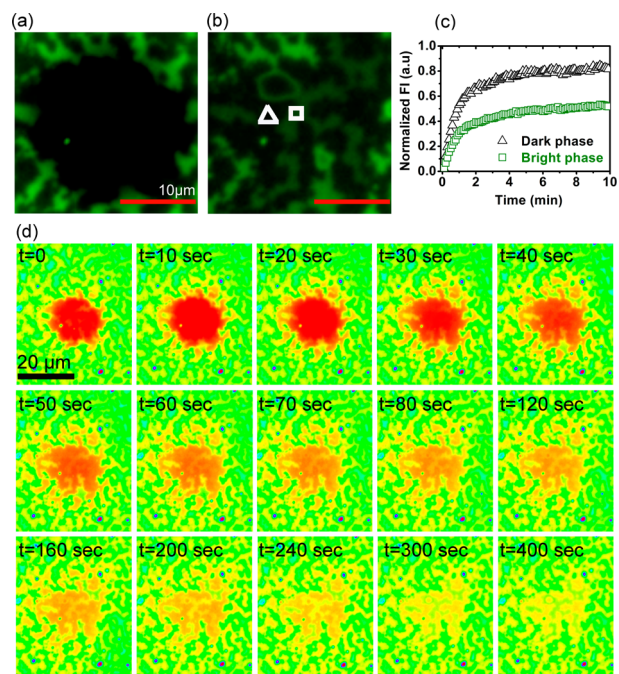


**Figure 3.** FRAP analysis of diffusion in stripe topography. (a, b) Enlarged views of a  $20 \mu\text{m}$  wide photobleached spot (a) immediately and (b) 10 min after a bleach pulse. (c) Recovery curves corresponding to the bright- and dark-phase areas indicated by the symbols in (b). (d) Sequence of false-color visualizations of FRAP images (bright phase, yellow; dark phase, green; bleached region, red).

In summary, the results presented here establish that supported membranes prepared by the SALB method enable direct characterization of coexisting liquid phases in the limit of high cholesterol concentration. At  $\sim 63$  mol % cholesterol, DOPC–Chol bilayers produce stripe superstructures consistent with that expected in the vicinity of the critical point for the  $\beta$  region in the phase diagram of the cholesterol/phospholipid mixtures.<sup>1d,e</sup> To the best of our knowledge, this is the first report of  $\beta$ -region phase separation in the supported bilayer system composed of lipid and cholesterol close to the solubility limit of cholesterol in fluid phase phospholipids such as DOPC.<sup>4b,c</sup> Moreover, these results also illustrate that the SALB approach offers a new tool to prepare supported membranes of arbitrary, predetermined compositions, enabling studies of biophysical characterization of complex membranes.

## ■ ASSOCIATED CONTENT

### 📄 Supporting Information

Experimental methods, supporting data, and videos S1–S3. This material is available free of charge via the Internet at <http://pubs.acs.org>.

## ■ AUTHOR INFORMATION

### Corresponding Authors

njcho@ntu.edu.sg  
anparikh@ucdavis.edu

### Notes

The authors declare no competing financial interest.

## ■ ACKNOWLEDGMENTS

We acknowledge support from the National Research Foundation (NRF-NRFF2011-01), the National Medical



Research Council (NMRC/CBRG/0005/2012), and NTU to N.J.C. Contributions by A.N.P. were supported by the Office of Basic Energy Sciences, U.S. Department of Energy (DE-FG02-04ER46173). J.A.J. is a recipient of the Nanyang President's Graduate Scholarship.

## ■ REFERENCES

- (1) (a) Leathes, J. B. *Lancet* **1925**, *1*, 853–856. (b) McConnell, H. M.; Vrljic, M. *Annu. Rev. Biophys. Biomol. Struct.* **2003**, *32*, 469–492. (c) McConnell, H. M.; Radhakrishnan, A. *Biochim. Biophys. Acta* **2003**, *1610*, 159–173. (d) Radhakrishnan, A.; McConnell, H. M. *Biophys. J.* **1999**, *77*, 1507–1517. (e) Radhakrishnan, A.; McConnell, H. M. *J. Am. Chem. Soc.* **1999**, *121*, 486–487. (f) Ege, C.; Ratajczak, M. K.; Majewski, J.; Kjaer, K.; Lee, K. Y. C. *Biophys. J.* **2006**, *91*, L1–L3. (g) Anderson, T. G.; McConnell, H. M. *Biophys. J.* **2002**, *83*, 2039–2052. (h) Honerkamp-Smith, A. R.; Cicuta, P.; Collins, M. D.; Veatch, S. L.; den Nijs, M.; Schick, M.; Keller, S. L. *Biophys. J.* **2008**, *95*, 236–246.
- (2) (a) Huang, J. Y.; Feigenson, G. W. *Biophys. J.* **1999**, *76*, 2142–2157. (b) Veatch, S. L.; Keller, S. L. *Phys. Rev. Lett.* **2002**, *89*, No. 268101. (c) Dietrich, C.; Bagatolli, L. A.; Volovyk, Z. N.; Thompson, N. L.; Levi, M.; Jacobson, K.; Gratton, E. *Biophys. J.* **2001**, *80*, 1417–1428.
- (3) (a) Stottrup, B. L.; Veatch, S. L.; Keller, S. L. *Biophys. J.* **2004**, *86*, 2942–2950. (b) Watkins, E. B.; Miller, C. E.; Liao, W. P.; Kuhl, T. L. *ACS Nano* **2014**, *8*, 3181–3191. (c) Ziblat, R.; Kjaer, K.; Leiserowitz, L.; Addadi, L. *Angew. Chem., Int. Ed.* **2009**, *48*, 8958–8961.
- (4) (a) Cremer, P. S.; Boxer, S. G. *J. Phys. Chem. B* **1999**, *103*, 2554–2559. (b) Buboltz, J. T.; Feigenson, G. W. *Biochim. Biophys. Acta* **1999**, *1417*, 232–245. (c) Huang, J.; Buboltz, J. T.; Feigenson, G. W. *Biochim. Biophys. Acta* **1999**, *1417*, 89–100.
- (5) (a) Hohner, A. O.; David, M. P. C.; Rädler, J. O. *Biointerphases* **2010**, *5*, 1–8. (b) Tabaei, S. R.; Choi, J. H.; Haw Zan, G.; Zhdanov, V. P.; Cho, N.-J. *Langmuir* **2014**, *30*, 10363–10373.
- (6) (a) Nielsen, L. K.; Bjornholm, T.; Mouritsen, O. G. *Nature* **2000**, *404*, 352–352. (b) Seul, M.; Andelman, D. *Science* **1995**, *267*, 476–483. (c) Veatch, S. L.; Soubias, O.; Keller, S. L.; Gawrisch, K. *Proc. Natl. Acad. Sci. U.S.A.* **2007**, *104*, 17650–17655.
- (7) Szoka, F.; Papahadjopoulos, D. *Proc. Natl. Acad. Sci. U.S.A.* **1978**, *75*, 4194–4198.
- (8) Subramaniam, A. B.; Guidotti, G.; Manoharan, V. N.; Stone, H. A. *Nat. Mater.* **2013**, *12*, 128–133.
- (9) Simonsson, L.; Höök, F. *Langmuir* **2012**, *28*, 10528–10533.
- (10) (a) Keller, C.; Kasemo, B. *Biophys. J.* **1998**, *75*, 1397–1402. (b) Sauerbrey, G. *Z. Phys.* **1959**, *155*, 206–222.
- (11) Jönsson, P.; Jonsson, M. P.; Tegenfeldt, J. O.; Höök, F. *Biophys. J.* **2008**, *95*, 5334–5348.
- (12) (a) Almeida, P. F.; Vaz, W. L.; Thompson, T. *Biochemistry* **1992**, *31*, 7198–7210. (b) Saxton, M. J. *Biophys. J.* **1994**, *66*, 394–401.